Performance Analysis of Diffusive Molecular Communication in Three Dimensional Channel

Prabhat Kumar Sharma and Lokendra Chouhan
Department of Electronics and Communication Engineering
Visvesvaraya National Institute of Technology Nagpur - 440010, India
(e-mail:prabhatmadhavec1@gmail.com, lokendrachouhan22@gmail.com)

***Abstract*—In this paper, we analyze the performance of the 3-dimensional diffusive molecular communication in terms of receiver operating characteristics, the average probability of error and capacity. The information is encoded through the number of molecules emitted from transmitter nanomachine, which follows the Brownian motion degrade over time, and reach at the spherical receiver nanomachine in random time. In this work, the expressions for the probability of detection, false alarm, the probability of error and capacity are derived. Our simulations show that the radius of the receiver has a strong effect over the receiver operating characteristic and the average probability of error, for considered system model. The expectancy of molecules have a great impact on the arrival probability in a 3-D environment and hence on the capacity of the considered system.**

***Index Terms*—Molecular communication, first hitting distribution, capacity, receiver operating characteristic (ROC).**

I. Introduction

Molecular communication is a nano-technology which attracts a biologist, a physicist, and a communication engineer for research [1]. Similar to the traditional communication system, molecular communication consist of transmitter nanomachines (TN), propagation medium and receiver nanomachines (RN). Recently molecular communication has gained more attention by bio-medical field for different applications such as nanomachines are used to transmit and gather information about malignant tumor inside the human body. The biological nanomachines have in-built sensing and actuating mechanism i.e., TN has the ability to actuate the transmission of information through molecules, by sensing the surrounding conditions. [2]. However, the information exchange is an important phenomenon for the identification of malignant tumor and send the drug to the target tumor without affecting healthy tissues. Hence, molecular communication has attracted significant research attention in recent years [3].

Authors in [4] modeled the channel and analyzed the capacity for the 1-D environment (1-D) for extended and naive modulations technique. The probability of error and capacity are also analyzed for M-ary and extended modulation schemes 1-D in [5]. The performance of direct diffusive molecular communication with mobile nanomachines is recently examined in terms of the ROC, the error probability and capacity [6]. In [7], relay assisted diffusion with drift based molecular communication system analyzed the probability of error considering the effect of inter-symbol-interference (ISI). In [8], the authors examined the different modulation techniques in terms of the bit-error-rate over time-varying channels considering 3-dimensional (3-D).

Till date, most of the researches focused on molecular communication in the 1-D environment where first hitting distribution for 1-D is used for analysis. However, the medium inside the blood capillary is 3-D space and molecules can travel in any direction. Therefore, it is more practical to consider the 3-D environment where RN is considered to be spherical with some finite radius. The expression for first hitting distribution for 3-D is derived in [9]. The authors in [10] also investigated the different types of receivers (active, passive, reversible adsorption and desorption receivers) in 1-D and 3-D environment. In our analysis, we use the first hitting distribution derived in [9].

To the best of our knowledge, none of the earlier works in the existing literature analyzed the probability of error and upper bound on the rate at which information can be reliably transmitted over a 3-D diffusive molecular communication channel. Hence, in this paper, we analyze the performance of molecular communication system in the 3-D environment in terms of ROC, capacity and the average probability of error. The closed form expressions of optimum threshold, probability of error and capacity are derived. We also consider the effect of practical disturbances such as multiple-source interference (MSI) and ISI at RN.

II. System Model

Consider a molecular communication system where a point TN and a spherical RN of radius r are placed in the 3-D environment as shown in Fig.1. Let d denotes the distance between TN and surface of the spherical RN. TN has the capability of the emitting fixed number of molecules which propagates in the aqueous environment with diffusion coefficient D_m. The RN assumed to be perfectly absorbing in nature and has an inbuilt mechanism of counting the number of molecules [1]. For transmission, amplitude shift keying (ASK) method is used i.e., M number of molecules are transmitted for bit 1 and, no molecules are transmitted for bit 0. The channel is divided into K number of time slots where information bits are

[1]The TN and RN assume to be perfectly synchronized.

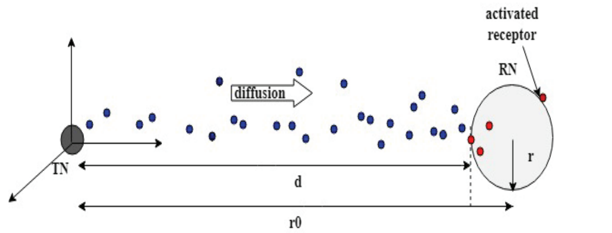

Fig. 1: Molecular communication system in 3-D scenario.

transmitted in each time slot for τ duration. If K denotes the total number of time slots, then jth time slot is defined as the time periods $[(j-1)\tau, j\tau]$, where $j \in \{1, 2, ...K\}$. The molecules emitted from TN follows the 3-D Brownian motion and propagate through the diffusion process and hit the RN surface. At RN after legend-receptor binding, activated receptor are counted and the corresponding symbol is detected [12]. At the beginning of each time-slot, the TN emits M molecules in the propagation medium with prior probability β for transmission of information symbol 1 or remains silent for transmission of information symbol 0. The molecules emitted from TN flow inside the aqueous environment get attenuated and have the life expectancy which follow the exponential distribution with degradation parameter γ. The density function for exponential distribution is given by

$$g(u) = \gamma e^{-\gamma u}, \tag{1}$$

where, u referred as the lifetime of molecules. The first hitting distribution for 3-D environment is already derived in [9] and is given by

$$f(t, i) = \frac{r}{r+d} \frac{d}{\sqrt{4\pi D_m t}} \exp\left(\frac{-d^2}{4D_m t}\right). \tag{2}$$

Due to the stochastic nature of the diffusive channel, the times of arrival at the RN of the molecules emitted by the TN, are random in nature and can span multiple time-slots. Let p_{j-i} denote the probability that molecules are transmitted in ith time-slot from TN and are arrived in jth time-slot at RN. The probability p_{j-i} can be derived using the first hitting time distribution [13] for mobile nanomachines as

$$p_m = p_{j-i} = \int_{(j-i)\tau}^{(j-i+1)\tau} f(t; i) \int_t^{\infty} g(u)\ du\ dt, \tag{5}$$

Let $N[j]$ is the total number of molecules received at RN in jth time-slot and is expressed as

$$N[j] = N_c[j] + N_I[j] + N_o[j], \tag{6}$$

where $N_c[j]$, is the number of molecules observed from current time-slot, which follows Binomial distribution $\mathcal{B}(Mx[j], p_0)$, where p_0 denotes the probability of arrival in the same time-slot. The quantity $N_I[j] = \sum_{i=1}^{j-1} N_I[i]$ denotes the ISI, i.e., number of molecules received from previous 1 to $(j-1)$ time-slots, where $N_I[i] \sim \mathcal{B}(Mx[j-i], p_i)$, with arrival probability of previous ith time slot p_i. The last term $N_o[j]$ denotes the MSI. For large number of molecules and small arrival probability, the Binomial distribution can be approximated well by Poisson distribution [14]. By applying Poisson approximation, the term $N_c[j]$ is approximated with average rate $\lambda_c[j] = Mx[j]p_0$, i.e., $N_c[j] \sim \mathcal{P}(Mx[j]p_0)$. Similarly, each term $N_I[i]$ in ISI can also be approximated as a Poisson distributed random variable i.e., $N_I[i] \sim \mathcal{P}(Mx[j-i]p_i)$. For MSI, we assume that the number of received unintended molecules for different time-slots are independent and no two unintended molecules are captured at same time [15]. Therefore, $N_o[j]$ also follows Poisson distribution with parameter $\lambda_o[j]$, i.e., $N_o[j] \sim \mathcal{P}(\lambda_o[j])$.

III. Detection Performance analysis

The symbol detection problem at the RN can be formulated as the binary hypothesis testing problem

$$\mathcal{H}_0 : N[j] = \sum_{i=1}^{j-1} N_I[i] + N_o[j], \tag{7}$$

$$\mathcal{H}_1 : N[j] = N_c[j] + \sum_{i=1}^{j-1} N_I[i] + N_o[j], \tag{8}$$

where $\mathcal{H}_0$ and $\mathcal{H}_1$ denote the null and alternative hypotheses corresponding to the transmission of symbol 0 and 1, respectively. Using the property of sum of independent Poisson distributed random variables, the number of molecules $N_[j]$ under $\mathcal{H}_0$ and $\mathcal{H}_1$ are distributed as,

$$\mathcal{H}_0 : \mathcal{P}(\lambda_0[j]), \qquad \mathcal{H}_1 : \mathcal{P}(\lambda_1[j]), \tag{9}$$

where, the parameters, $\lambda_0[j] = \sum_{i=1}^{j-1} x[j-i]Mp_i + \lambda_o[j]$ and $\lambda_1[j] = Mp_0 + \sum_{i=1}^{j-1} x[j-i]Mp_i + \lambda_o[j]$. Further to find optimum threshold at RN log- likelihood-ratio-test (LLRT) can be formulated as

$$\log\left[\frac{Pr[N[j]]|\mathcal{H}_1}{Pr[N[j]]|\mathcal{H}_0}\right] \underset{\mathcal{H}_0}{\overset{\mathcal{H}_1}{\gtrless}} \log\left[\frac{1-\beta}{\beta}\right], \tag{10}$$

where, using the Poisson distributions under $\mathcal{H}_1$ and $\mathcal{H}_0$

$$p(N[j]|\mathcal{H}_1) = \frac{e^{-\lambda_1[j]}(\lambda_1[j])^{N[j]}}{N[j]!}, \tag{11}$$

$$p(N[j]|\mathcal{H}_0) = \frac{e^{-\lambda_0[j]}(\lambda_0[j])^{N[j]}}{N[j]!}. \tag{12}$$

Now the optimal decision rule at the RN can be obtained as, $N[j] \underset{\mathcal{H}_0}{\overset{\mathcal{H}_1}{\gtrless}} \eta[j]$, where the optimal threshold $\eta[j]$ is given by

$$\eta[j] = \frac{\ln(1/\beta - 1) + \big(\lambda_1[j] - \lambda_0[j]\big)}{\ln(\lambda_1[j]) - \ln(\lambda_0[j])}, \tag{13}$$

Let $X[j]$ and $Y[j]$ be two discrete random variables that represent the transmitted and received symbols in the jth time-slot respectively.

Then detection probability ($P_D[j]$) and false alarm probability ($P_{FA}[j]$) at RN are

$$P_D[j] = \Pr(y[j]=1|x[j]=1) = 1 - \sum_{l=1}^{\lfloor \eta[j] \rfloor} \frac{e^{-\lambda_1[j]}(\lambda_1[j])^l}{l!}. \tag{14}$$

$$
\begin{aligned}
I(X[j],Y[j]) &= \left[\Pr(y[j]=0|x[j]=0)\Pr(x[j]=0)\times\log_2\frac{\Pr(y[j]=0|x[j]=0)}{\Pr(y[j]=0)}\right]+\left[\Pr(y[j]=1|x[j]=0)\times\Pr(x[j]=0)\right.\\
&\quad\left.\times\log_2\frac{\Pr(y[j]=1|x[j]=0)}{\Pr(y[j]=1)}\right]+\left[\Pr(y[j]=0|x[j]=1)\times\Pr(x[j]=1)\times\log_2\frac{\Pr(y[j]=0|x[j]=1)}{\Pr(y[j]=0)}\right]\\
&\quad+\left[\Pr(y[j]=1|x[j]=1)\times\Pr(x[j]=1)\times\log_2\frac{\Pr(y[j]=1|x[j]=1)}{\Pr(y[j]=1)}\right], \qquad (3)\\
&=\left[(1-P_{FA}[j])(1-\beta)\log_2\frac{(1-P_{FA}[j])}{\Pr(y[j]=0)}\right]+\left[P_{FA}[j](1-\beta)\log_2\frac{P_{FA}[j]}{\Pr(y[j]=1)}\right]\\
&\quad+\left[(1-P_D[j])\beta\log_2\frac{(1-P_D[j])}{\Pr(y[j]=0)}\right]+\left[P_D[j]\beta\log_2\frac{P_D[j]}{\Pr(y[j]=1)}\right], \qquad (4)
\end{aligned}
$$

$$P_{FA}[j]=\Pr(y[j]=1|x[j]=0)=1-\sum_{l=1}^{\lfloor\eta[j]\rfloor}\frac{e^{-\lambda_0[j]}(\lambda_0[j])^l}{l!}. \quad (15)$$

where $\lfloor\alpha\rfloor$ gives the largest integer less than or equal to α.

IV. Average probability of error and capacity

The expression for probability of error for jth time slot is derived as follows

$$
\begin{aligned}
P_e[j] &= \Pr(y[j]=0|x[j]=1)\Pr(x[j]=1)\\
&\quad+\Pr(y[j]=1|x[j]=0)\Pr(x[j]=0), \qquad (16)
\end{aligned}
$$

using (14)-(15), $P_e[j]$ can be written as

$$P_e[j]=(1-P_D[j])\ \beta+P_{FA}[j]\ (1-\beta). \quad (17)$$

The average probability of error can be written as

$$\bar{P}_e=\frac{1}{K}\sum_{j=1}^{K}P_e[j]. \quad (18)$$

Let $X[j]$ and $Y[j]$ be two discrete random variables that represent the transmitted and received symbols in the jth time-slot respectively. The channel capacity is found by maximizing the end to end mutual information in each time slots. The mutual information between $X[j]$ and $Y[j]$ can be obtained as

$$
\begin{aligned}
I(X[j],Y[j]) &= \sum_{x[j]\in\{0,1\}}\sum_{y[j]\in\{0,1\}}\Pr(y[j]|x[j])\\
&\quad\times\Pr(x[j])\log_2\frac{\Pr(y[j]|x[j])}{\Pr(y[j])}, \qquad (19)
\end{aligned}
$$

The eq. (19) is simplified in eq. (3)-(4). where,

$$
\begin{aligned}
\Pr(y[j]=0) &= \Pr(y[j]=0|x[j]=0)\Pr(x[j]=0)\\
&\quad+\Pr(y[j]=0|x[j]=1)\Pr(x[j]=1)\\
&=(1-P_{FA}[j])(1-\beta)+(1-P_D[j])\beta, \qquad (20)
\end{aligned}
$$

Similarly,

$$\Pr(y[j]=1)=P_{FA}[j](1-\beta)+P_D[j]\beta. \quad (21)$$

Using the above results with number of time slots $K\to\infty$ [13], the capacity of a diffusive molecular communication channel in 3-D environment can be obtained by maximizing the mutual information $I(X[j],Y[j])$ as

$$C[j]=\max_{\beta}(I(X[j],Y[j])\quad\text{bits/slot}, \quad (22)$$

for the given values of $P_{FA}[j]$ and $P_D[j]$ in jth time slot, the capacity is obtained by maximizing the $I(X[j],Y[j])$ as a function of prior probability β. Differentiating Eq. (4) with respect to the prior probability β and equating zero

$$H(P_{FA}[j])-H(P_D[j])+(P_D[j]-P_{FA}[j])\log_2(\frac{q_0[j]}{q_1[j]})=0, \quad (23)$$

where, $H(a)$ is binary entropy function and defined as, $H(a)=-a\log_2(a)-(1-a)\log_2(1-a)$. Also, $q_0[j]=\Pr(y[j]=0)$ and $q_1[j]=\Pr(y[j]=1)$. Using (23) the expression of prior probability β_m at maximum mutual information is derived as

$$\beta_m=\frac{P_{FA}[j]\left(2^{\frac{H(P_D[j])-H(P_{FA}[j])}{P_D[j]-P_{FA}[j]}}+1\right)-1}{(P_{FA}[j]-P_D[j])\left(2^{\frac{H(P_D[j])-H(P_{FA}[j])}{P_D[j]-P_{FA}[j]})}+1\right)}, \quad (24)$$

The closed form expression for the channel capacity is derived using (4) and (24) as follows

$$C[j]=H(q_0[j])-(1-\beta_m)H(P_{FA}[j])-\beta_m H(P_D[j]). \quad (25)$$

V. Numerical Results

In this section, we numerically analyze the system using Monte-Carlo simulations for 10^5 samples. The system

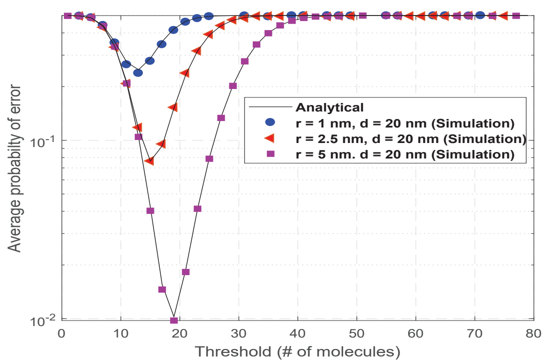

Fig. 2: $\bar{P}_e$ vs η.

parameters are chosen such that the number of molecules M and the arrival probability p_m satisfy the Binomial to Poisson approximation conditions, i.e., $Mp_m<10$.

Fig. 2 shows the average probability of error performance as a function detection threshold for different values of radius of spherical RN. For the simulations, the parameters are chosen as: $K = 5$, $M = 100$, $d = 20$ nm, $\lambda_o[j] = 10, \forall j$, $\gamma = 10$, $\beta = 0.5$ and $D_m = 5 \times 10^{-10}$ m^2/s. The parameters remain same until unless stated. Two observations can be made, first, is that the average probability of error achieves its lower bound at optimum threshold value $\eta[j]$. Second, for the large value of r the lower-bound of $\bar{P}_e$ is less, compare to the case when the value of r is small. For example at $r = 2.5$ nm the lower-bound of $\bar{P}_e$ is .085, while, at $r = 1$ nm the lower-bound of $\bar{P}_e$ increases to 0.25.

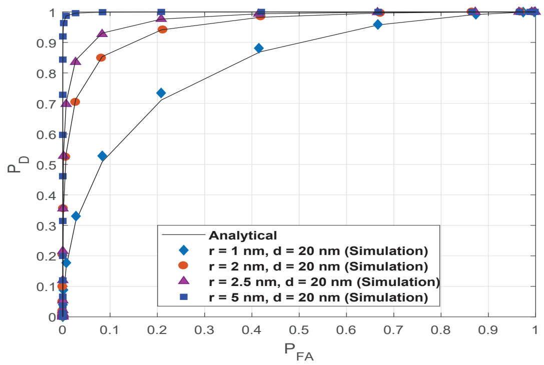

Fig. 3: ROC curve.

Fig. 3 shows the ROC curve for different values of radius of the spherical receiver. One can observe that increase in the radius of spherical RN at fixed values of probability of false alarm results increase in detection probabilities. At $r = 5$ nm the area under the ROC is close to 1, which infer that the detection performance improves with an increase in the radius of RN. This is due to the fact that, for high values of r, the hitting probability of molecules increases.

The capacity against the time-slot duration at different values of r analyzed in Fig. 4. To obtain the capacity in each time slot, the values of $P_D[j]$ and $P_{FA}[j]$ are obtained. The capacity is obtained by maximizing the mutual information about priory probability β. The system parameters chosen are, $K = 10$, $M = 500$, $d = 20$ nm, $\lambda_o[j] = 10, \forall j$, $\gamma = 1$, and $D_m = 5 \times 10^{-8}$ m^2/s. It can be observed that, as the time-slot duration increases the capacity improves significantly and achieves floor for high time-slot duration. One can also observe that at high values of r, the system achieves significant capacity gain. This is due to the fact that the arrival probability p_m increases with the radius of the RN.

VI. Conclusion

In this paper, the performance of 3-D molecular communication is analyzed in terms of ROC, the average probability of error and capacity. The closed-form expressions of the probability of detection, false alarm and the average probability of error and channel capacity are derived considering the practical disturbances in the channel. The life expectancy of molecules is also considered during analysis. The novel expression for the optimum threshold is also derived. Simulation results are perfectly matched with all the numerical results we have developed. Future work may be the focus over analysis mobile molecular communication considering the 3-D environment.

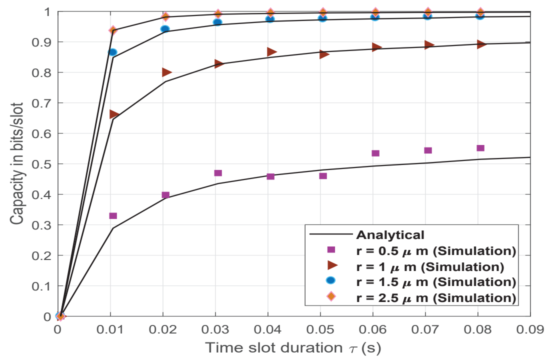

Fig. 4: Capacity of 3-D molecular communication system vs time slot duration

References

[1] T. Nakano, M. J. Moore, F. Wei, A. V. Vasilakos, and J. Shuai, "Molecular communication and networking: Opportunities and challenges," *IEEE Trans. Nanobiosci.*, vol. 11, no. 2, pp. 135–148, 2012.

[2] N. Farsad, H. B. Yilmaz, A. Eckford, C.-B. Chae, and W. Guo, "A comprehensive survey of recent advancements in molecular communication," *IEEE Commun. Surveys Tuts.*, vol. 18, no. 3, pp. 1887–1919, 2016.

[3] T. Nakano, A. W. Eckford, and T. Haraguchi, *Molecular Communication*. Cambridge University Press, 2013.

[4] T. Nakano, Y. Okaie, and J. Liu, "Channel model and capacity analysis of molecular communication with brownian motion," *IEEE Communications Letters*, vol. 16, no. 6, pp. 797–800, June 2012.

[5] A. Singhal, R. K. Mallik, and B. Lall, "Performance analysis of amplitude modulation schemes for diffusion-based molecular communication," *IEEE Trans. on Wireless Commun.*, vol. 14, no. 10, pp. 5681–5691, Oct 2015.

[6] N. Varshney, A. K. Jagannatham, and P. K. Varshney, "On diffusive molecular communication with mobile nanomachines," in *Proc. 52nd Annual CISS*, March 2018, pp. 1–6.

[7] N. Tavakkoli, P. Azmi, and N. Mokari, "Performance evaluation and optimal detection of relay-assisted diffusion-based molecular communication with drift," *IEEE Trans. on NanoBiosci.*, vol. 16, no. 1, pp. 34–42, Jan 2017.

[8] B. C. Akdeniz, M. C. Gursoy, A. E. Pusane, and T. Tugcu, "On the performance of the modulation methods in time-varying molecular communication channels," in *2017 40th International Conference on Telecommunications and Signal Processing (TSP)*, July 2017, pp. 128–131.

[9] H. B. Yilmaz, A. C. Heren, T. Tugcu, and C. Chae, "Three-dimensional channel characteristics for molecular communications with an absorbing receiver," *IEEE Communications Letters*, vol. 18, no. 6, pp. 929–932, June 2014.

[10] I. Isik, H. B. Yilmaz, and M. E. Tagluk, "A preliminary investigation of receiver models in molecular communication via diffusion," in *2017 International Artificial Intelligence and Data Processing Symposium (IDAP)*, Sept 2017, pp. 1–5.

[11] M. Pierobon and I. F. Akyildiz, "A statistical physical model of interference in diffusion-based molecular nanonetworks," *IEEE Transactions on Communications*, vol. 62, no. 6, pp. 2085–2095, June 2014.

[12] A. Einolghozati, M. Sardari, and F. Fekri, "Capacity of diffusion-based molecular communication with ligand receptors," in *2011 IEEE Information Theory Workshop*, Oct 2011, pp. 85–89.

[13] T. Nakano, Y. Okaie, and J. Q. Liu, "Channel model and capacity analysis of molecular communication with Brownian motion," *IEEE Commun. Lett.*, vol. 16, no. 6, pp. 797–800, June 2012.

[14] T.T.Soong, *Fundametlas of Probability and Statistics for Engineers*, 2004.

[15] Y. K. Lin, W. A. Lin, C. H. Lee, and P. C. Yeh, “Asynchronous threshold-based detection for quantity-type-modulated molecular communication systems,” *IEEE Trans. Mol. Biol. Multi-Scale Commun.*, vol. 1, no. 1, pp. 37–49, March 2015.